Superabsorbent Polymeric Materials. XII. Effect of Montmorillonite on Water Absorbency for Poly(Sodium Acrylate) and Montmorillonite Nanocomposite Superabsorbents

Wen-Fu Lee, Lin-Gi Yang

Department of Chemical Engineering, Tatung University, Taipei, Taiwan, Republic of China

ABSTRACT: A series of novel xerogels based on sodium acrylate (NaA), montmorillonite (MMT), and N,N'-methylene-bisacrylamide (NMBA) were prepared by inverse suspension polymerization and water solution polymerization. The influences of pure MMT, intercalated MMT, the method of polymerization, and the content of the MMT in the copolymeric gels on the water absorbency and the initial absorption rate in deionized water and various salt solutions were investigated. Results showed that the water absorbency was increased by adding a small amount of the pure MMT into the copolymeric gels, but decreased by adding intercalated MMT into the gels. In addition, the water absorbency of the gels prepared by water solution polymerization was lower than that prepared by inverse suspension polymerization.© 2004 Wiley Periodicals, Inc. J Appl Polym Sci 92: 3422–3429, 2004

Key words: superabsorbent; montmorillonite; nanocomposite

INTRODUCTION

Superabsorbent polymers are water-insoluble, hydrogel-forming polymers capable of absorbing large amounts of aqueous fluids and retaining the absorbed fluids even under pressure. Therefore, superabsorbents have great advantages over traditional water-absorbing materials. Because of their excellent characteristics, superabsorbents are widely used in many fields, such as disposable diapers, feminine napkins, soil for agriculture and horticulture, gel actuators, water-blocking tapes, medicine for the drug delivery system, absorbent pads, etc.[1–8] Many researchers attempted to modify these absorbent polymers to enhance their absorbency, gel strength, and absorption rate after the first superabsorbent polymer was reported by the U.S. Department of Agriculture in 1961.[9–24]

In recent years, the study of organic–inorganic nanocomposites has become a very important field. Currently, reinforcing polymer with small amounts of smectite clays has attracted increasing interest because the derived heterostructural materials exhibit impressive mechanical, thermal, optical, and other properties that increase their technological value.[25–30]

Incorporating montmorillonite (MMT) into superabsorbent polymer and fabricating a composite is significant in reducing the product cost and improving the water absorbency of superabsorbent materials. In this study, the influences of different methods for preparing poly(sodium acrylate)/MMT nanocomposites and the effect of intercalated MMT on the water absorbency of the nanocomposite superabsorbent were investigated.

EXPERIMENTAL

Materials

Acrylic acid (AA), which was purified by vacuum distillation at 63°C/25 mmHg, and N,N'-methylene-bisacrylamide (NMBA) as a crosslinking agent, were obtained from Aldrich Co. (St. Louis, MO). Sodium hydroxide, (3-Acrylamidopropyl) trimethylammonium chloride (TMAACl), purchased from Tokyo Kasei Industries Ltd. (Tokyo, Japan), and NMBA were used directly as received. 4,4'-Azobis(4-cyanovaleric acid) (ACVA) as an initiator and sorbitan monostearate (Span 60) as a stabilizer were also purchased from Tokyo Kasei Industries Ltd. Methanol and cyclohexane (Katayama Chemicals, Osaka, Japan) were of reagent analytical grade.

Preparation of NaA monomer solution

Sodium acrylate (NaA) monomer was prepared as reported previously.[31]

TABLE I
Feed Compositions of NaA/Montmorillonite Xerogels Obtained from Inverse Suspension and Water Solution Polymerization

Sample codes	NaA (g)	Na$^+$-MMT (g)	TMAACL-MMT (g)	NMBA (g)	Yield (%)
HA0	20	0	0	0.07	94.5
NB2	20	0.41	—	0.07	88.6
NB4	20	0.83	—	0.07	82.33
NB6	20	1.28	—	0.07	85.75
IB2	20	—	0.41	0.07	83.55
IB4	20	—	0.83	0.07	79.2
IB6	20	—	1.28	0.07	77.8
SB2	20	—	0.41	0.07	92.33
SB4	20	—	0.83	0.07	94.8
SB6	20	—	1.28	0.07	89.6

NB series, inverse suspension.
IB series, inverse suspension.
SB series, water solution polymerization.

Purification and intercalation of MMT

To prepare Na$^+$-exchanged MMT, 5 g of clay was suspended in 200 mL NaCl solution with a concentration of 1M. The suspension solution was stirred for 5 h at room temperature. In this process, Na$^+$-MMT was generated. The suspension solution containing Na$^+$-MMT was centrifuged. The Na$^+$-MMT was washed four times with 2 L of water to remove excess NaCl. Finally, the Na$^+$-MMT was dried in a vacuum oven at 35°C for 3 days.

Quaternary alkylammonium-exchanged MMT was synthesized as follows: the suspension solution, containing 5 g of Na$^+$-MMT and 1.64 g of TMAACl, was mixed in 500 mL of water and stirred at 70°C for 1 day. Then, the TMAACl-MMT was separated by centrifugation and washed with large volumes of water to remove unreacted TMAACl and residual NaCl. The sample was dried in a vacuum oven at 35°C.

Preparation of sodium acrylate and MMT nanocomposite superabsorbent polymer

Inverse suspension polymerization

A 300-mL four-necked separable flask equipped with a reflux condenser, a stirring rod, and a thermometer was charged with 65 mL cyclohexane and 0.2 g Span 60. The mixture was stirred until Span 60 was dissolved (continuous phase).

The crosslinking agent, NMBA, and the appropriate amount of Na$^+$-MMT or TMAACl-MMT were introduced into NaA monomer solution and the mixture was stirred until the NMBA was dissolved completely. The monomer solution and 0.15 g initiator, ACVA (dispersion phase), were introduced into the reactor. Air was flushed from the reactor by introducing nitrogen until the entire process was completed. The stirrer speed was maintained at 400 rpm. The polymerization was set at 70°C for 4 h. After polymerization, the suspension solution was cooled and then precipitated by 800 mL cold methanol under stirring. The product was filtered and washed several times by a mixture of water and methanol (1 : 9 in volume). The product was then dried in a vacuum oven at 100°C for 1 day. A white powdered polymer was obtained. The feed compositions of samples are listed in Table I.

Water solution polymerization

The crosslinking agent, NMBA, and the appropriate amount of TMAACl-MMT were introduced into a 300-mL four-necked separable flask equipped with a reflux condenser, a stirring rod, and a thermometer. NaA monomer solution and the mixture were stirred until the NMBA was dissolved completely. The NaA monomer solution and 0.15 g initiator, ACVA (dispersion phase), were introduced into the flask. Air was flushed from the flask by introducing nitrogen until the entire process was completed. The stirrer speed was maintained at 400 rpm. The polymerization was set at 70°C for 4 h. After polymerization, the polymerization mixture was cooled and then precipitated by 800 mL cold methanol under stirring. The product was filtered and washed several times by the mixture of water and methanol (1 : 9 in volume). The product was then dried in a vacuum oven at 100°C for 1 day. A white powdered polymer was obtained. The feed compositions of samples are listed in Table I.

X-ray diffraction analysis

Powder XRD analyses were performed by using a MAC Sienco X-ray powder diffractometer with Cu anode (model M21X, Osaka, Japan), running at 40 kV and 30 mA, scanning from 3° to 13° at 3°/min. The
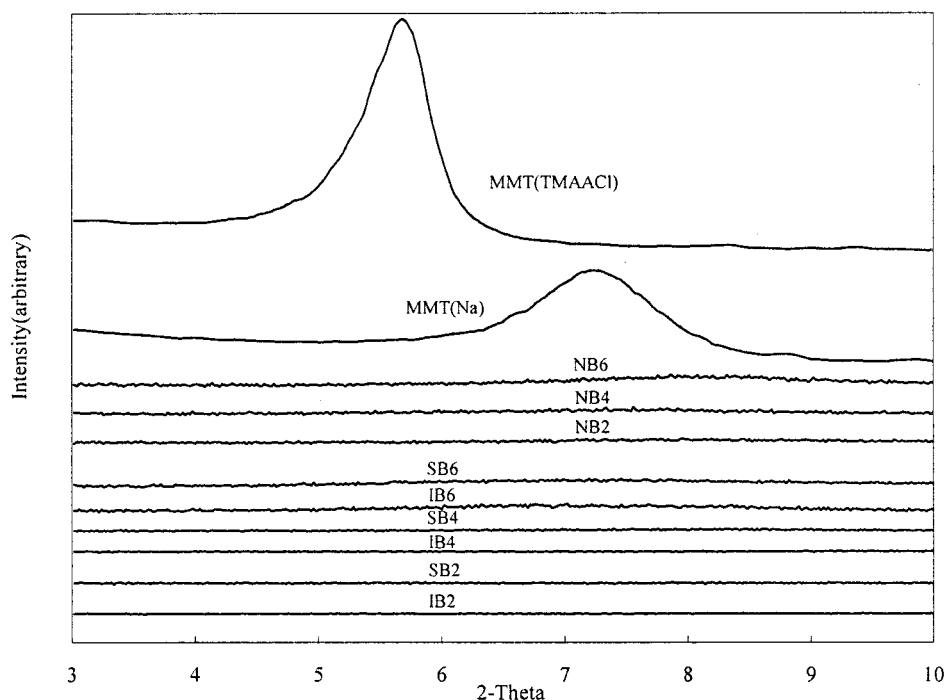
Figure 1 The XRD patterns of Na$^+$-MMT and TMAACl-MMT, and various nanocomposite gels.

structure of the MMT was determined at different stages of the nanocomposite synthesis. The MMT powders were mounted on a sample holder with a large cavity, and a smooth surface was obtained by pressing the powders with a glass plate. Analyses of the TMAACl-MMT in the swollen gels were performed by spreading the mixture on a gel membrane disc (50 mm diameter, 0.5 mm thick) used as sample holder. It was designed so that a maximum surface could be irradiated at a low angle, giving an optimum intensity to the XRD signal. The nanocomposite plates produced during the molding process had a fairly smooth surface.

Measurement of property

All samples were dried in a vacuum oven at 100°C before any tests. All of the samples were used with a particle size in the range of 65–100 mesh.

Morphology

The dried specimens were examined for morphological details by using scanning electron microscopy (SEM; JEOL JXA8600, Tokyo, Japan) with an acceleration voltage of 15 kV. The specimens were coated with a gold metal layer to provide proper surface conduction.

Measurement of water absorbency

Suction filtration method

The samples (50 mg) were immersed in an excess of deionized water or 0.9 wt % NaCl$_{(aq)}$ for at least 8 h to

reach swelling equilibrium at room temperature; the residual water was removed by suction filtration with an aspirator (250 mmHg) for 15 min. The gel was weighed and the equilibrium absorbency Q_{eq} was calculated by

$$Q_{eq} = \frac{W_{wet} - W_{dry}}{W_{dry}} \qquad (1)$$

where W_{dry} is the weight of the dried sample and W_{wet} is the weight of the swollen sample.

Tea bag method

The tea bag was made of 250-mesh nylon screen. The tea bag containing the sample (50 mg) was immersed entirely in deionized water or the saline solution and kept there until swelling equilibrium and then hung up for 25 min to drain the excess solution and weighed. The equilibrium absorbency was calculated by eq. (1).

Absorbency in various saline solutions

The samples (50 mg) were immersed in an excess of various saline solutions with different concentrations (NaCl$_{(aq)}$, CaCl$_{2(aq)}$, FeCl$_{3(aq)}$), retained there for at least 8 h, and then filtered with suction and weighed. The water absorbency in the above saline solution was obtained.
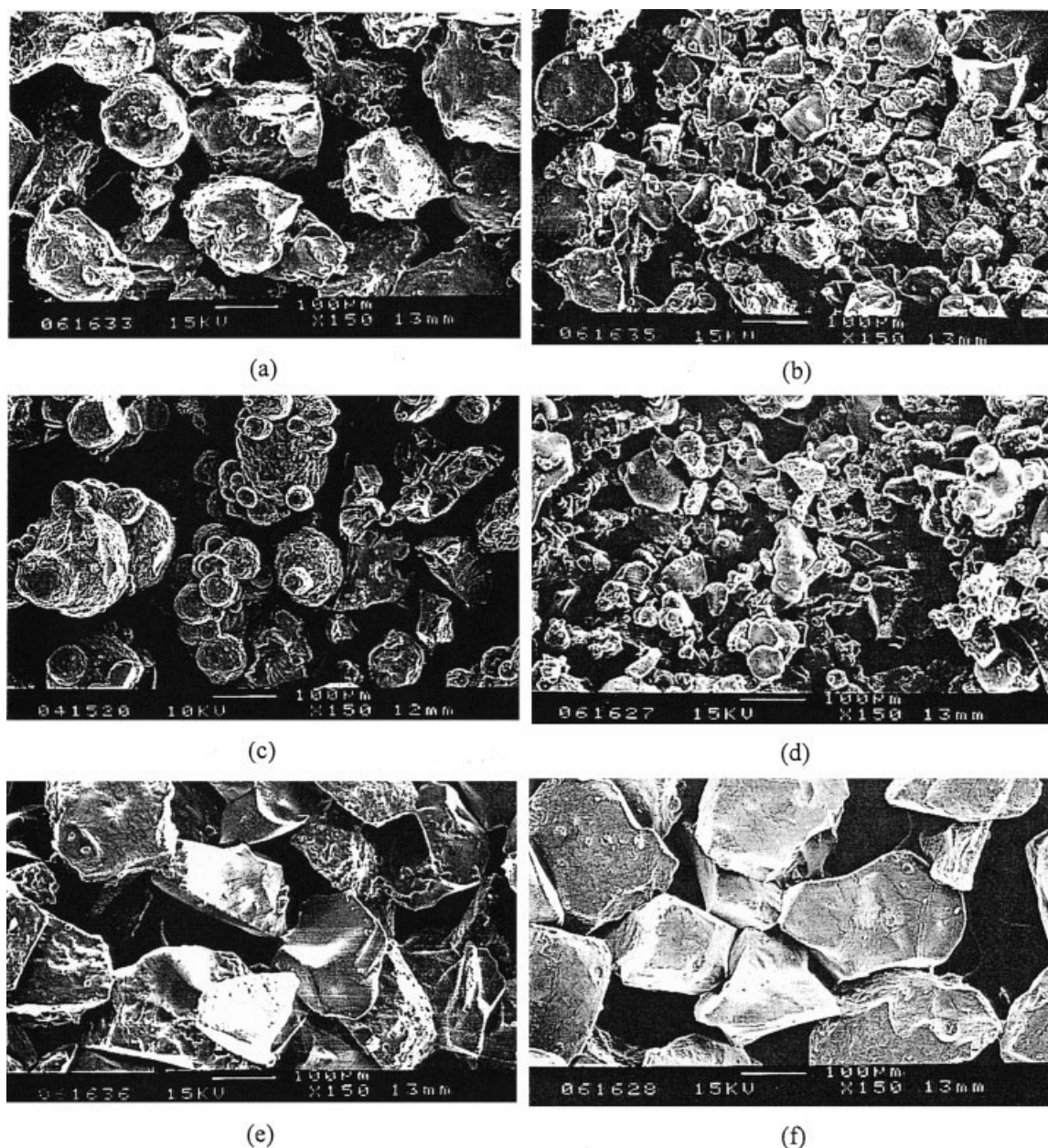
Figure 2 Scanning electron micrographs for dried NB series gels (a)–(b), IB series gels (c)–(d), and SB series gels (e)–(f), ×150.

Kinetics of swelling

A technique based on the demand wettability (DW) method was adopted. A graduated burette with an air inlet at the bottom was linked by a flexible tube to a plate covered with a metallic grid (250 mesh). After filling with the saline solution, the burette was closed at the top and air was introduced while the xerogel absorbed water. The sample (50 mg) of absorbent was placed on the grid, and the swelling kinetics were easily measured. The absorbency at every time interval was calculated by

$$Q = \frac{V_s \times d_{H_2O}}{W_d} \qquad (2)$$

where Q is the characteristic absorbency, V_s is the absorbed volume, d_{H2O} is the density of water, and W_d is the weight of the dry sample.

RESULTS AND DISCUSSION

Identification of the nanocomposite hydrogels

The XRD patterns of Na$^+$-MMT, TMAACl-MMT, and various nanocomposite gels were plotted and are shown in Figure 1. From Figure 1, a typical diffraction pattern of Na$^+$-MMT was evident with a strong peak corresponding to a basal spacing of 12.3 Å. After intercalation with TMAACl, this peak was shifted to a low angle, corresponding to basal spacing of 15.5 Å.
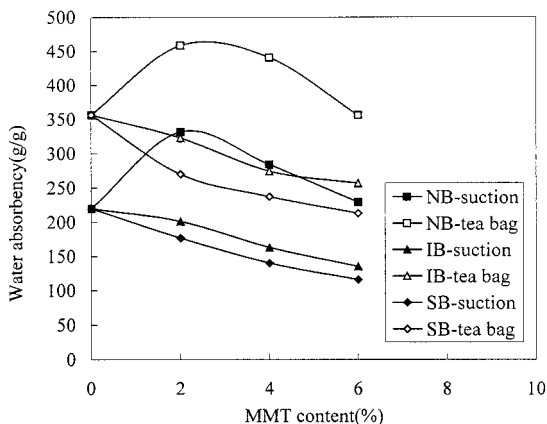
Figure 3 Effect of Na$^+$-MMT content for NB, IB, and SB series gels on water absorbency in deionized water by tea-bag method and suction method.

This indicated that the TMAACl ions have intercalated the layers during the cation-exchange process adopting a lateral bilayer structure. After polymerization with Na$^+$-MMT and intercalated MMT, the diffraction peaks were not observed from Figure 1. This suggests that, in the poly(NaA/Na$^+$-MMT) and the poly(NaA/intercalated MMT), the MMT minerals were exfoliated.

SEM

The microphotographs of the particles for three series of nanocomposite superabsorbents observed from SEM are shown in Figure 2. As shown in these figures, the particles obtained from inverse suspension polymerization approach a spherical shape and some aggregates occur [see Fig. 2(c, d)], but the particles prepared from water solution polymerization were irregular in shape and showed a larger size [see Fig. 2(e, f)].
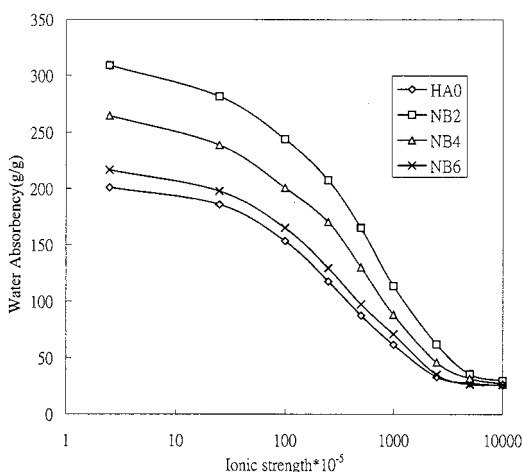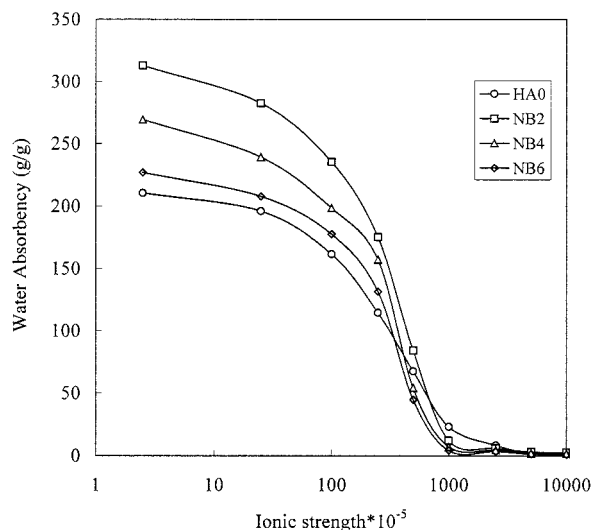

Figure 5 Water absorbency of the poly(NaA/Na$^+$-MMT) gels in the CaCl$_{2(aq)}$ with various ionic strengths.

This different shape will affect their water absorption behavior.

Effect of Na$^+$-MMT content on water absorbency in deionized water

The water absorbency in deionized water measured by suction filtration and the tea bag method as a function of the content of Na$^+$-MMT in the copolymeric gels is shown in Figure 3 (NB-series). The results showed that the water absorbency increased with an increase in a small amount of MMT. According to Flory's theory,[32] the water absorbency of a gel is dependent on ionic osmotic pressure, crosslinking density, and the affinity of the gel for water. In low Na$^+$-MMT content (2 wt %), Na$^+$-MMT is easily ionized and dispersed into poly(NaA) gels. This enhances
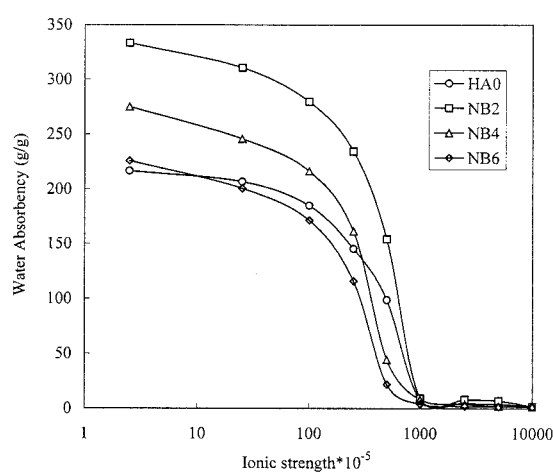

Figure 4 Water absorbency of the poly(NaA/Na$^+$-MMT) gels in the NaCl$_{(aq)}$ with various ionic strengths.

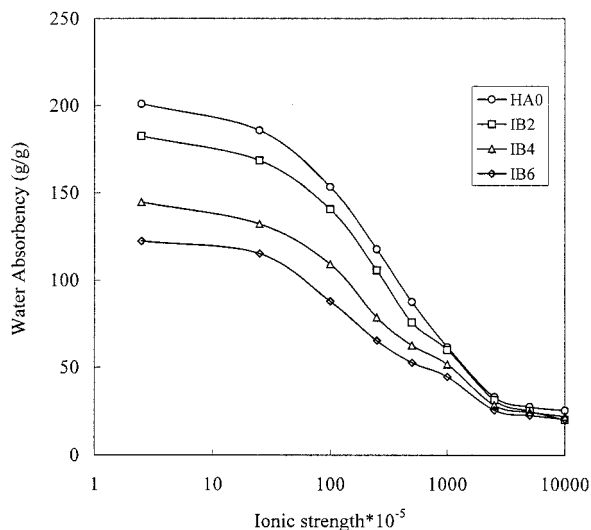**Figure 6** Water absorbency of the poly(NaA/Na$^+$-MMT) gels in the FeCl$_{3(aq)}$ with various ionic strengths.

Figure 7 Water absorbency of the poly(NaA/TMAACl-MMT) gels obtained from inverse suspension polymerization in the $NaCl_{(aq)}$ with various ionic strengths.

the hydrophilicity of poly(NaA) gels and makes it swell more. However, at higher Na^+-MMT contents, above 2 wt %, the water absorbency decreases with an increase of Na^+-MMT. The water absorbency of the nanocomposite gels is affected not only by the affinity of the gel for water but also by the interaction between the network and the clay. This suggests that interaction occurs between hydroxyl groups on the surface of MMT and carboxyl groups on the NaA.[33]

In addition, the water absorbencies in deionized water measured by suction filtration and the tea bag method as a function of the content of TMAACl-MMT in the copolymeric gels through inverse suspension polymerization and water solution polymerization are
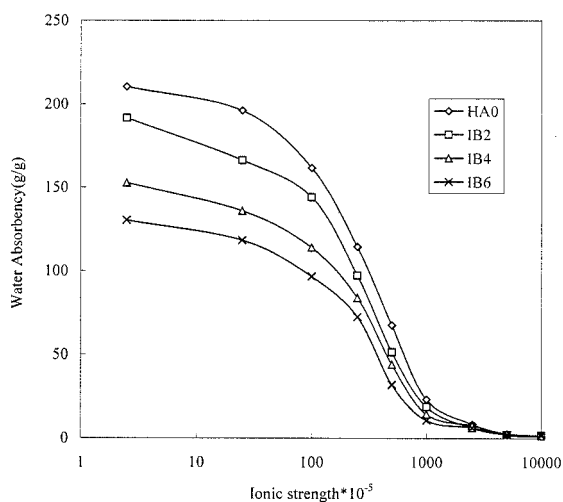

Figure 8 Water absorbency of the poly(NaA/TMAACl-MMT) gels obtained from inverse suspension polymerization in the $CaCl_{2(aq)}$ with various ionic strengths.

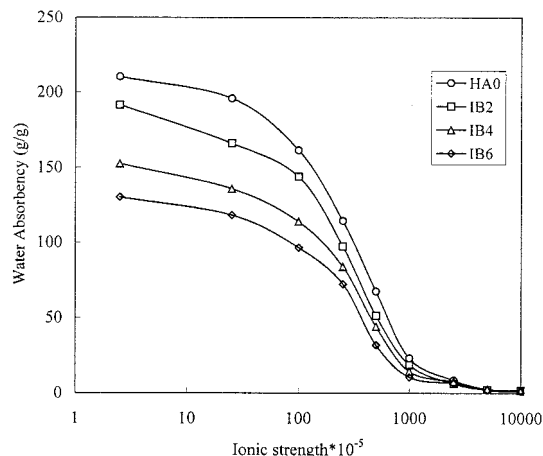**Figure 9** Water absorbency of the poly(NaA/TMAACl-MMT) gels obtained from inverse suspension polymerization in the $FeCl_{3(aq)}$ with various ionic strengths.

shown in Figure 3(IB and SB), respectively. The water absorbencies in these figures decrease with an increase in the amount of TMAACl. This is because the sodium ion of Na^+-MMT was exchanged by the TMAACl ion and resulted in no ions to ionize; the other reason is that interaction occurs between OH groups on the surface of MMT and COO^- groups on the NaA. This resulted in the shrinkage of the gels.

Furthermore, these figures also indicate that the water absorbency of the copolymeric gels prepared by water solution polymerization were lower than inverse suspension polymerization. Inspecting the microphotographs of SEM, the particle sizes prepared from water solution polymerization were visibly larger and irregular in shape. The result indicated that the gels aggregated during polymerization. Based on this reason, the structure of the nanocomposite gels
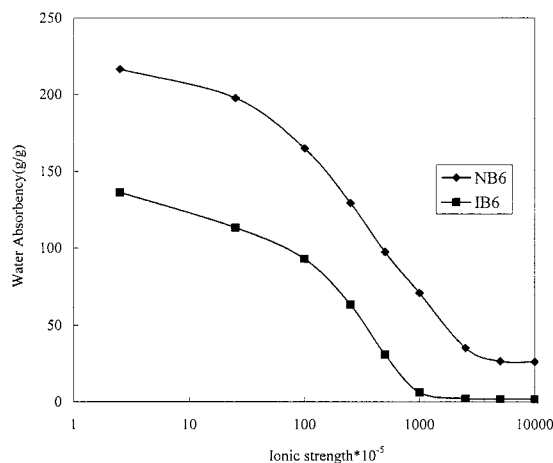

Figure 10 Water absorbency of sample 6 wt % of the different copolymeric gels in the $CaCl_{2(aq)}$ with various ionic strengths.
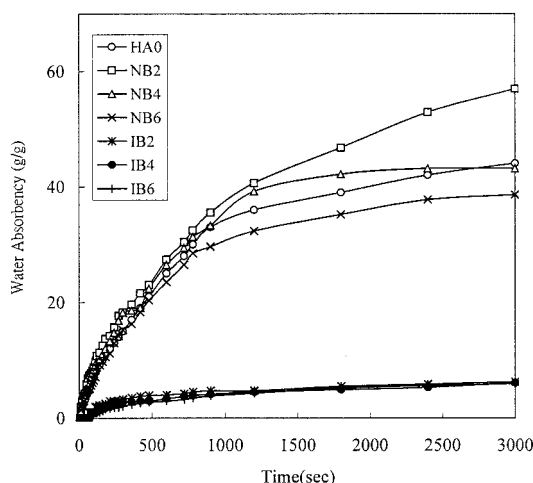
Figure 11 Absorption rate in deionized water for the poly(NaA/Na$^+$-MMT) and poly(NaA/TMAACl-MMT) gels by DW method.

prepared by water solution polymerization is tighter than for those gels prepared by inverse suspension polymerization.

Water absorbency in various saline solutions

The water absorbencies for the NB-series and IB-series copolymeric gels as a function of different ionic strengths for $NaCl_{(aq)}$, $CaCl_{2(aq)}$, and $FeCl_{3(aq)}$ are shown in Figures 4-6 and 7-9, respectively. In addition, the water absorbency for NB6 and IB6 copolymeric gels in different ionic strength for $CaCl_{2(aq)}$ is shown in Figure 10.

These figures show that the water absorbencies for the copolymeric gels in various salt solutions decrease with increasing of the ionic strength of salt solutions. This can be attributed to the cations in the salt solution such as Na$^+$, Ca^{2+}, and Fe^{3+}: the cation would neutralize the carboxylate group. The difference in ionic osmotic pressure between the gel and the external solution reduces with an increase of the ionic strength of the salt solutions. Hence, the water absorbency decreases when the ionic strength in the external solution increases. The curves of water absorbency for monovalent cationic salt solution also were flatter than those for divalent and trivalent cationic salt solutions. The water absorbency converged to 0 when those gels

were immersed into high ionic strength divalent and trivalent cationic salt solutions (see Figs. 5–6, 8–9), but not for monovalent cationic salt solution (see Figs. 4 and 7). This is because the divalent calcium ion (Ca^{2+}) and trivalent ferric ion (Fe^{3+}) would form complexes with the carboxylate group. On the other hand, the tendency of water absorbency for the NB-series gels and IB-series gels in various saline solutions is similar to the tendency for those gels in deionized water (compare Figs. 4–9 with Fig. 3).

In addition, the result in Figure 10 indicates that the curve of water absorbency for the IB6 gel was flatter than that for the NB6 gel in the $CaCl_{2(aq)}$. This is because the Na$^+$-MMT is easily ionized and the cations of salt ions would easily absorb on the surface of MMT. Thus, the decreased range of the water absorbency for the NB6 gel was larger than that for the IB6 gel.

Effect of MMT content on absorption rate for the copolymeric gels

Buchanan et al.[34] has suggested that the swelling kinetic for the absorbent is significantly influenced by swelling capacity, size distribution of powder particles, specific surface area, and apparent density of the polymer.

Figure 11 shows the absorption rate in deionized water for NB-series and IB-series copolymeric gels. The characteristic absorption data of these two series of gels are shown in Table II. The results shown in Table II indicate that the tendency of the initial absorption rate is in the order NB2 > NB4 > NB6 ≫ IB2 ≒ IB4 ≒ IB6. From SEM micrographs, the appearance of Na$^+$-MMT series gels was similar to TMAACl-MMT series gels. So the swelling ratio depends on the affinity of the gels for water. Because the water absorbency of TMAACl-MMT series gels was too low, the initial absorption rate was very small. For Na$^+$-MMT series gels, Na$^+$-MMT are easily ionized in low Na$^+$-MMT content, and this enhances the hydrophilicity of the gels.

CONCLUSION

From above results, conclusions can be drawn as follows: the water absorbency was increased by adding a

TABLE II
Absorption Characteristics for NaA/Na$^+$-MMT Copolymeric Gels Systems in Deionized Water

Conditions	HA0	NB2	NB4	NB6	IB2	IB4	IB6
Initial absorption rate (Q/min)							
30 s	5.20	7.84	6.10	5.88	0	0	0
30 s–1 min	4.00	5.88	4.85	3.06	0	0	0
1–3 min	3.20	2.94	3.38	3.86	1.25	0.88	0.75

small amount of the Na^+-montmorillonite into the copolymeric gels, but decreased by adding intercalated montmorillonite into the gels. In addition, the water absorbency of the copolymeric gels, obtained from water solution polymerization, was lower than that of those gels from inverse suspension polymerization. However, the water absorbency of these gels decreased with an increase in the ionic strength of external salt solution. The decreased range of the water absorbency for the poly(NaA/Na^+-MMT) was larger than that for the poly(NaA/TMAACl-MMT). The initial absorption rate was increased with an increase of Na^+-MMT content in the gels.

References

1. Buchholz, F. L. in Superabsorbent Polymers: Science and Technology; Buchholz, F. L.; Peppas, N. A., Eds.; ACS Symposium Series 573; American Chemical Society: Washington, DC, 1994.
2. Sakiyama, T.; Chu, C. H.; Fujii, T.; Yano, T. J Appl Polym Sci 1993, 50, 2021.
3. Yoshida, M.; Asano, M.; Kumakura, M. Eur Polym Mater 1989, 25, 1197.
4. Shiga, T.; Hirose, Y.; Okada, A.; Kurauchi, T. J Appl Polym Sci 1992, 44, 249.
5. Shiga, T.; Hirose, Y.; Okada, A.; Kurauchi, T. J Appl Polym Sci 1993, 47, 113.
6. Hogari, K.; Ashiya, F. Advances in Superabsorbent Polymers; American Chemical Society: Washington, DC, 1994.
7. Ericksen, P. H.; Nguyen, H. V.; Oczkowski, B.; Olejnik, T. A. Eur. Pat. 40,087, 1981.
8. Kobayashi, T. Kobunshi 1987, 36 (8), 612.
9. U.S. Department of Agriculture U.S. Pat. 3,981,100, 1961.
10. Taylor, N. W.; Fanta, G. F.; Doane, W. M.; Russell, C. R. J Appl Polym Sci 1978, 22, 1343.
11. Burr, R. C.; Fanta, G. F.; Doane, W. M. J Appl Polym Sci 1979, 27, 2713.
12. Fanta, G. F.; Burr, R. C.; Doane, W. M.; Russell, C. R. J Appl Polym Sci 1979, 24, 1384.
13. Kejun, Y.; Berlian, W. J Appl Polym Sci 1990, 41, 3079.
14. Fanta, G. F.; Burr, R. C.; Doane, W. M. J Appl Polym Sci 2015 1979, 24.
15. Yoshinobu, M.; Morita, M.; Sakata, I. J Appl Polym Sci 1992, 45, 805.
16. Lokhande, H. T.; Varadarjan, P. V.; Iyer, V. J Appl Polym Sci 2031 1992, 45.
17. Zoda, I. Funct Mater 1986, 6, 76.
18. Isomi, K. Jpn. Pat. 56, 707, 1989.
19. Nagasuna, K.; Suminaga, N.; Kimura, K.; Shimonura, T. Jpn. Pat. 126,234, 1989.
20. Imada, H.; Fujiwaka, M. Jpn. Pat. 141,938, 1989.
21. Fujio, A.; Komae, T.; Yutaka, Y. Jpn. Pat. 210,463, 1989.
22. Yada, S.; Shibano, T.; Ito, K. Jpn. Pat. 215,801, 1990.
23. Sano, M.; Mikamo, H.; Suehiro, T.; Wakabayashi, N. Jpn. Pat 258,839, 1991.
24. Sakiyama, T.; Chu, C. H.; Fujii, T.; Yano, T. J Appl Polym Sci 1993, 50, 2021.
25. Aranda, P.; Ruiz-Hitzky, E. Appl Clay Sci 1999, 15, 119.
26. Giammels, E. P. Adv Mater 1996, 8, 29.
27. Fournaris, K. G.; Karakassides, M. A.; Yiannakopoulou, K.; Petridis, D. Chem Mater 1999, 11, 2372.
28. Kojima, Y.; Usuki, A.; Kawasumi, M.; Okada, A.; Fukushima, Y.; Kurauchi, T.; Kamigaito, O. J Mater Res 1993, 8, 1185.
29. Krishnamoorti, R.; Vaia, R. A.; Giannelis, E. P. Chem Mater 1996, 8, 1728.
30. Lagaly, G. Appl Clay Sci 1999, 15, 1.
31. Lee, W. F.; Yang, L. G. J Appl Polym Sci to appear.
32. Flory, P. J. Principles of Polymer Chemistry; Cornell Univ. Press: Ithaca, NY, 1953.
33. Wu, J. H.; Lin, J. M.; Li, G. Q.; Wei, C. G. Polym Int 2001, 50, 1050.
34. Buchanan, K. J.; Hird, B.; Letcher, T. M. Polym Bull 1986, 15, 325.